The formation mechanism of voids in physical vapor deposited AlN epilayer during high temperature annealing

Cite as: Appl. Phys. Lett. **116**, 251601 (2020); https://doi.org/10.1063/5.0012792
Submitted: 05 May 2020 . Accepted: 10 June 2020 . Published Online: 22 June 2020

Jianwei Ben, Zhiming Shi, Hang Zang, Xiaojuan Sun, Xinke Liu, Wei Lü, and Dabing Li

Applied Physics Letters ARTICLE scitation.org/journal/apl

The formation mechanism of voids in physical vapor deposited AlN epilayer during high temperature annealing

Cite as: Appl. Phys. Lett. **116**, 251601 (2020); doi: 10.1063/5.0012792
Submitted: 5 May 2020 · Accepted: 10 June 2020 ·
Published Online: 22 June 2020

Jianwei Ben,[1,2] Zhiming Shi,[1,3] Hang Zang,[1,3] Xiaojuan Sun,[1,3] Xinke Liu,[2] Wei Lü,[1,4,a)] and Dabing Li[1,3,a)]

AFFILIATIONS

[1]State Key Laboratory of Luminescence and Applications, Changchun Institute of Optics, Fine Mechanics and Physics, Chinese Academy of Sciences, 3888 Dong Nan Hu Road, Chang Chun 130033, People's Republic of China
[2]Information Engineering, Guangdong Research Center for Interfacial Engineering of Functional Materials, Shenzhen University-Hanshan Normal University Postdoctoral Workstation and College of Physics and Optoelectronic Engineering, Shenzhen University, Shenzhen 518060, China
[3]Center of Materials Science and Optoelectronics Engineering, University of Chinese Academy of Sciences, Beijing 100049, China
[4]Key Laboratory of Advanced Structural Materials, Ministry of Education and Advanced Institute of Materials Science, Changchun University of Technology, Changchun 130012, China

[a)]**Authors to whom correspondence should be addressed:** lw771119@hotmail.com and lidb@ciomp.ac.cn

ABSTRACT

The voids will be formed in the physical vapor deposited (PVD)-AlN epilayer after high temperature annealing. In this work, the formation mechanism of voids and its effect on crystal quality are investigated. Based on microstructural analysis and first principles calculations, it is confirmed that (1) the dislocations mainly gather around the voids and the strain status around the voids is similar to other regions in the same PVD-AlN epilayer, (2) the paired dislocations with opposite signs prefer to move closer and react with each other during high temperature annealing, thus contributing to the formation of voids, (3) the voids provide the inner surface for dislocations to terminate, decreasing the density of the threading dislocation propagating to the surface, and (4) the emergence of dislocations is energetically favorable and the energy dropped by 5.93 eV after the two isolated dislocation lines fused into a void by overcoming a barrier of 1.34 eV. The present work is of great significance for improving the quality and performance of AlN materials and devices.

As an ultrawide bandgap semiconductor, AlN is receiving great attention due to its excellent properties such as the direct band structure, high breakdown voltage, and polarization characteristics, showing potential applications in deep ultraviolet photoelectronic and power electronic devices.[1–10] Due to the deficiency of the AlN homogenous substrate, great efforts have been dedicated to heteroepitaxy growth of AlN on substrates such as sapphire, SiC, and Si.[11–14] The intrinsic physical difference between AlN and heterogeneous substrate materials, such as the lattice mismatch and thermal mismatch, would result in high dislocation density in the AlN epitaxy layer. Although several effective methods have been developed to grow AlN on heterogeneous substrates, such as epitaxial lateral overgrowth, migration-enhanced epitaxy, and ammonia (NH_3) pulse-flow growth,[15–17] achieving high-quality AlN using a facile but effective method was still challenging. Fortunately, the high temperature (HT) annealing method developed in 2016 has been proven to be an effective method to obtain high-quality AlN material using a simple process and with high repeatability.[18] Several groups have investigated the HT annealing method, and some interesting phenomena were reported such as the polarity inversion and higher compressive stress in HT-annealed AlN.[19–21] However, it has been reported that the voids would be formed in the physical vapor deposited (PVD)-AlN epilayer after HT annealing,[19] and there is no detailed investigation for understanding the formation mechanism of the voids during HT annealing, which is extremely important for the stable growth of high-quality AlN wafers and fabricating devices.

Herein, the formation mechanism of the voids and its effect on crystal quality are systematically investigated and clarified. It is found that the distance between different dislocations will be shortened to form paired dislocations during HT annealing, and the reaction

between the paired dislocations contributes to the formation of voids, which is energetically favorable compared to dislocation migration. The voids will further attract the dislocations to gather around them and can also provide the inner surface for dislocations to terminate, decreasing the density of the threading dislocation propagating to the surface.

At first, about 60 nm-thickness AlN was sputtered on c-sapphire substrates at 650 °C in a N_2 atmosphere under 4 mTorr using an AlN Sputter system with equipment model: iTops A230. Then, 600 nm AlN epilayers was grown via metal-organic chemical vapor deposition at 1277 °C under the pressure of 40 mbar to fabricate AlN templates. Trimethylaluminum and NH_3 were used as precursor gases. The templates were annealed at 1500 °C and 1700 °C 1 h in a N_2 atmosphere to improve the crystal quality.

The dislocation density of the AlN templates decreased from $2.78 \times 10^9\,cm^{-2}$ to $1.81 \times 10^9\,cm^{-2}$ for 1500 °C annealing and $5.39 \times 10^8\,cm^{-2}$ for 1700 °C annealing according to the x-ray diffraction (XRD) results shown in Fig. S1 and Table S1, supplementary material, indicating that the HT annealing could effectively improve the quality of the AlN epilayer. The microstructure evolution of samples with different HT annealing temperatures is shown in Fig. 1. Figure 1(a) shows the high-resolution transmission electron microscope (HRTEM) cross-sectional view of the AlN sample without annealing, and no void could be found. For samples annealed at 1500 °C and 1700 °C as shown in Figs. 1(b) and 1(c), the formation of voids in the PVD layer is confirmed, and the voids are hexagonal in shape and have regular edges.

It is generally considered that the voids could relax the strain in AlN that suffered from the heterogeneous substrate.[22,23] Here, the HRTEM images are shown in Fig. 2 to analyze the strain status around the voids. The HRTEM images are taken along the $(11\bar{2}0)$ plane of AlN. The crystalline interplanar spacing is calculated by the peak-finding method as shown in Figs. 2(d) and 2(e), and the detailed calculations are given in the supplementary material and Fig. S2. 12 points in different regions are chosen, the corresponding strains are calculated for the three samples, and the results are listed in Table S2, supplementary material. For the sample without annealing, the strain distribution is inhomogeneous due to the high density of grain boundaries. For the annealed samples, from the overall view, it is unexpectedly found that the stress status around the voids does not show obvious difference with other regions in the same PVD AlN template. To further confirm the results, the Geometric phase analysis (GPA) images are taken to exhibit the strain field around the voids as shown in Figs. 2(f) and 2(g), which exhibits the strain field for the region in the dotted line in Figs. 2(b) and 2(c), respectively. From the extracted strain data on the right side of Figs. 2(f) and 2(g), it can be concluded that the strain variation is in permeable error limits at the edge of the voids compared to that of the regions outside the voids.

These results strongly indicate that the strains around the voids are the same as those of other regions. The dislocation distribution is an important indication to analyze strain. The distribution of dislocations around the voids is confirmed by the fringe images for samples without and with 1700 °C annealing as shown in Fig. 3, and the fringe images for the sample with 1500 °C annealing are shown in Fig. S3, supplementary material. For the sample without annealing, a region in the PVD-AlN layer is selected randomly because there is no evident difference among different regions in PVD-AlN before annealing. For

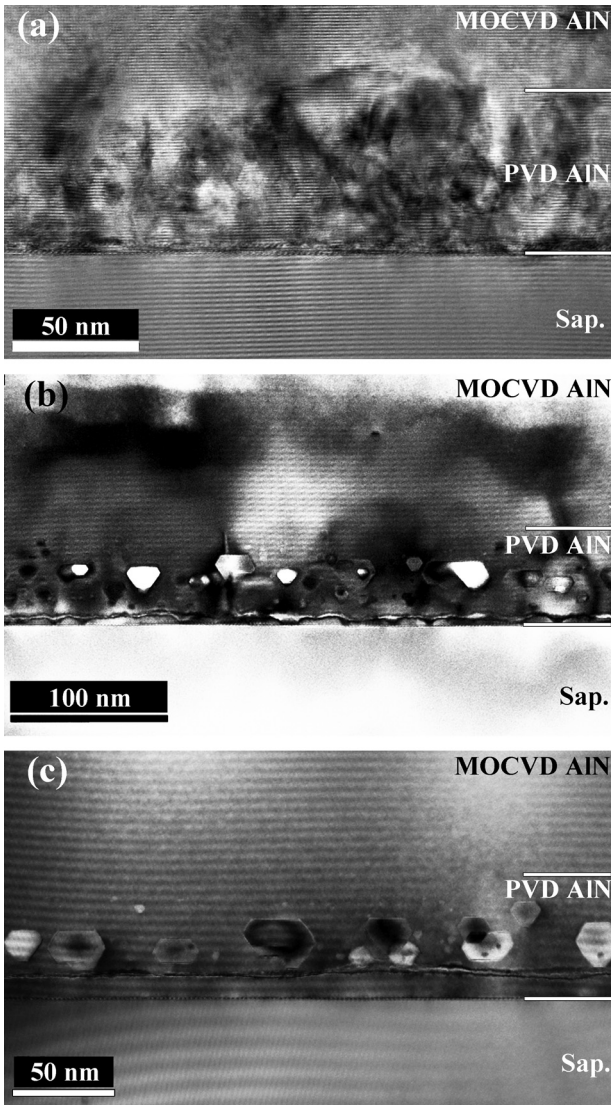

FIG. 1. The cross-sectional TEM images of AlN templates without annealing (a), with 1500 °C annealing (b), and with 1700 °C annealing (c).

the sample with 1700 °C annealing, two regions in the PVD-AlN layer are selected, one is at the edge of the void and the other is away from the void. As the Burgers vectors of screw and edge dislocations in AlN are $\langle 0001 \rangle$ and $1/3\ \langle 11\bar{2}0 \rangle$,[24,25] the fringe images of (0001) and $(11\bar{2}0)$ planes are extracted and the dislocations are marked in Figs. 3(d)–3(f) and 3(h)–3(j), respectively. For the PVD-AlN template without annealing, the distribution of dislocations is irregular as shown in Figs. 3(d) and 3(h). After 1700 °C annealing, there is no observable dislocation along both (0001) and $(11\bar{2}0)$ planes for the position away from the void as shown in Figs. 3(f) and 3(j), and the dislocations are mainly gathered around the edge of the void as shown in Figs. 3(e) and 3(i). With the aggregation of dislocations, the probability of the interaction between dislocations will be greatly increased, resulting in the dislocation annihilation and formation dislocation loop as shown

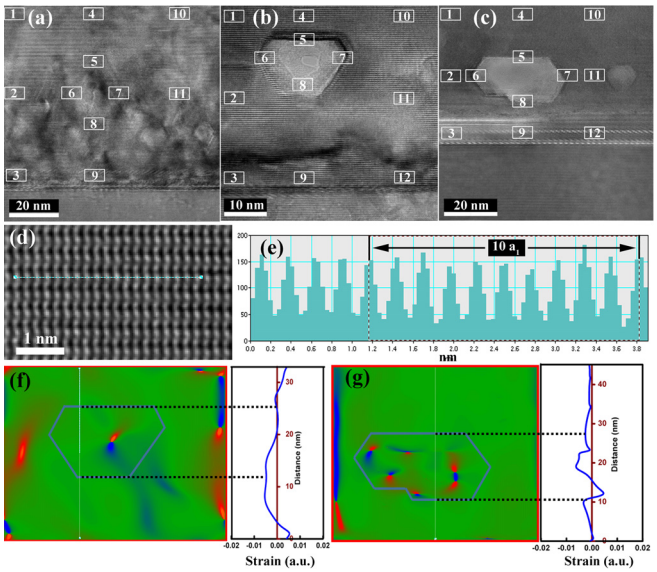

FIG. 2. The cross-sectional HRTEM images of AlN epilayers along the (11-20) direction without annealing (a), with 1500 °C annealing (b), and with 1700 °C annealing (c); (d) the detailed view of the part of HRTEM results; the blue line is the path to read the lattice parameter; (e) the example of how the peak-finding method works to obtain the lattice parameter along the path in (d). (f) and (g) the GPA images and the extracted strain along the thin line of the void region in (b) and (c), respectively. The white rectangles marked with numbers in (a)–(c) are the area for reading lattice parameters. The lattice parameters of the numbered area are extracted, and the compressive strains are summarized in Table S2.

in the black circle in Fig. 3(e).[26] It is also found that the direction of the Burgers vector of one dislocation is always accompanied by the other nearby dislocation with the opposite Burgers vector, inducing the strain cancelation around dislocation by each other, which explains why although there is a high dislocation density around the void, the strain around the void is not significantly different with other areas in the same sample. From the above analysis, it can be concluded that the voids will attract the dislocations to conglomerate and increase the reaction possibility of dislocations to annihilate or form dislocation loops. Accordingly, the density of the threading dislocation propagating to the surface could be decreased as indicated by XRD results.

To illustrate the formation mechanism of the voids, the dislocation evolution model combined theoretical analysis is constructed and shown in Fig. 4. The dislocations with different signs will slip toward each other under the influence of external energy such as temperature; the II part in Fig. 4(a) is the most common pattern that formed around the voids after HT annealing, and the II-i part is the HRTEM image taken from Fig. 3(e), showing the dislocation behavior descripted above. The atomic mechanism of the behavior of dislocations is further investigated by the molecular dynamics (MD) simulation and first-principles calculations. At high temperature, the calculated distance between the two dislocation lines decreases quickly, indicating that there is an attracting interaction between the two dislocation lines with opposite burgers vectors, and the atomic trajectory shows that the dislocation line tends to migrate along the slipping plane parallel to the Burgers vector. As shown in Fig. 4(b), the high temperature can offer extra energy to overcome the migration barrier (1.76 eV), which is induced by 60° rotation for the Al-N pair (marked by the green

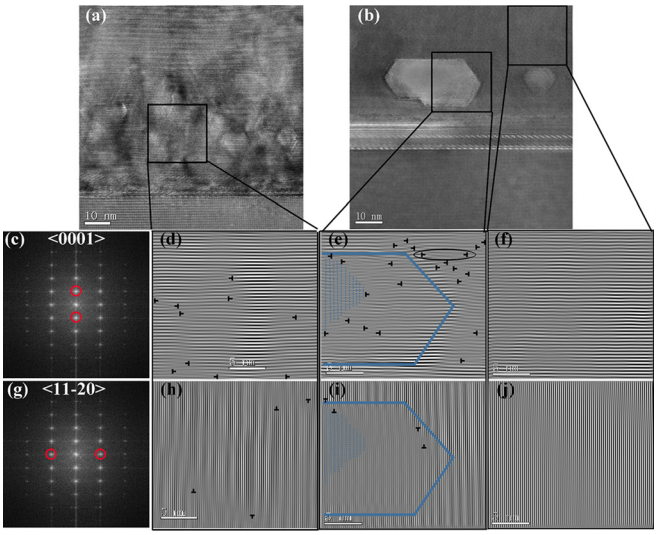

FIG. 3. The cross-sectional HRTEM images of AlN epilayers without annealing (a) and with 1700 °C annealing (b), and the marked squares are the areas to be taken for Fourier and inverse Fourier analysis; (c) and (g) are the FFT results for the selected area, and the red circle means the selected crystal orientation; (d)–(f) the fringe image of the (0001) plane of the corresponding area; (h)–(j) the fringe images of the (11-20) plane of the corresponding area. The dislocations are marked in (d)–(f) and (h)–(j); the solid blue lines in (e) and (f) are the contour of the void, while the dotted blue line overwrites the region that is foggy.

circle). However, the situation for dislocation mergence is entirely different, and the energy sharply dropped by 5.93 eV after the two isolated dislocation lines fused into a bigger void by overcoming a barrier of 1.34 eV. It demonstrated that the bigger void is energetically

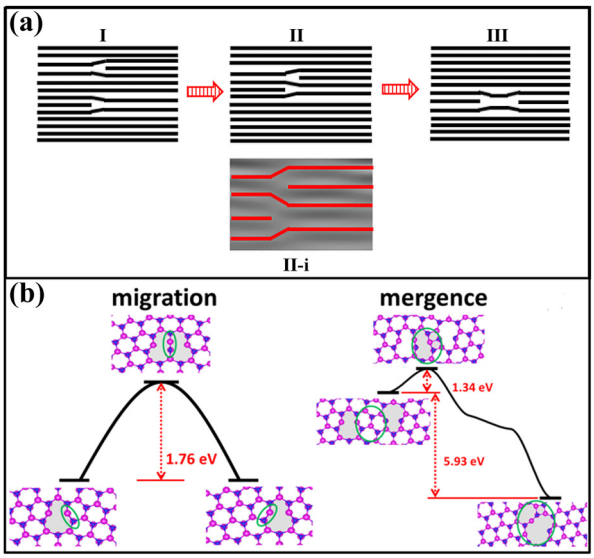

FIG. 4. The evolution of the dislocations with the different signs with high temperature annealing. (a) The experimental model of the movement of dislocations. I part represents the original positions of dislocations; II part shows the movement of dislocations during HT annealing, and II-i is the corresponding TEM results extracted from Fig. 3(e); III part is the further reaction of part II. (b) The atomic evolution of migration and emergence of dislocations by simulation.

favorable. Once the voids are formed, they will further attract the dislocations to gather around them according to the experimental results. Based on the theoretical simulation, the volume of the void will be increased with higher annealing temperature because higher energy will be provided to promote the dislocations merging into the void, which is consistent with the experimental phenomena. The average width of the voids after 1500 °C annealing is 16.88 nm, while the average width is 23.19 nm for AlN with 1700 °C annealing. The density of dislocations and grain boundaries will be greatly decreased during this process.

In summary, the formation mechanism of voids in the PVD AlN epilayer after HT annealing and its effect on crystal quality are investigated and clarified in the present work. It is found that the void will attract dislocations to move toward and gather around it. The shortened distance between neighboring dislocations with different signs will increase the possibility for dislocations to annihilate and form dislocation loops. The voids are formed via the emergence of dislocations with different signs and will further attract dislocations to merge into it, leading to the higher volume of the voids with higher annealing temperature. The voids are beneficial to lower the dislocation outcrop density, which is of great significance to further AlN epitaxy and fabricate devices.

See the supplementary material for XRD data and Table S1, calculation of the strain and Table S2, and the fringe images of the PVD-AlN epilayer with 1500 °C annealing.

This work was supported by the National Science Fund for Distinguished Young Scholars (No. 61725403), the National Key R&D Program of China (No. 2016YFB0400101), the National Natural Science Foundation of China (Nos. 61574142, 61874118, 61827813, and 61704171), the Key Program of the International Partnership Program of CAS (No. 181722KYSB20160015), the Jilin Provincial Science and Technology Department (No. 20180201026GX), and the Youth Innovation Promotion Association of CAS.

DATA AVAILABILITY

The data that support the findings of this study are available from the corresponding author upon reasonable request.

REFERENCES

[1]B. Ren, M. Liao, M. Sumiya, J. Li, L. Wang, X. Liu, Y. Koide, and L. Sang, J. Alloys Compd. **829**, 154542 (2020).
[2]X. Liu, H. Wang, H. C. Chiu, Y. Chen, D. Li, C. R. Huang, H. L. Kao, H. C. Kuo, and S. H. Chen, J. Alloys Compd. **814**, 152293 (2020).
[3]T. A. Growden, W. Zhang, E. R. Brown, D. F. Storm, D. J. Meyer, and P. R. Berger, Light **7**, 17150 (2018).
[4]P. Reddy, M. H. Breckenridge, Q. Guo, A. Klump, D. Khachariya, S. Pavlidis, W. Mecouch, S. Mita, B. Moody, J. Tweedie, R. Kirste, E. Kohn, R. Collazo, and Z. Sitar, Appl. Phys. Lett. **116**, 081101 (2020).
[5]A. Ding, L. Kirste, Y. Lu, R. Driad, N. Kurz, V. Lebedev, T. Christoph, N. M. Feil, R. Lozar, T. Metzger, O. Ambacher, and A. Žukauskait, Appl. Phys. Lett. **116**, 101903 (2020).
[6]D. Y. Kim, J. H. Park, J. W. Lee, S. Hwang, S. J. Oh, J. Kim, C. Sone, E. F. Schubert, and J. K. Kim, Light **4**, e263 (2015).
[7]D. Li, X. Sun, H. Song, Z. Li, Y. Chen, H. Jiang, and G. Miao, Adv. Mater. **24**, 845 (2012).
[8]Y. Mei, G. Weng, B. Zhang, J. Liu, W. Hofmann, L. Ying, J. Zhang, Z. Li, H. Yang, and H. Kuo, Light **6**, e16199 (2017).
[9]D. Li, K. Jiang, X. Sun, and C. Guo, Adv. Opt. Photonics **10**, 43 (2018).
[10]Y. Taniyasu and M. Kasu, Appl. Phys. Lett. **96**, 221110 (2010).
[11]B. K. SaifAddin, A. S. Almogbel, C. J. Zollner, F. Wu, B. Bonef, M. Iza, S. Nakamura, S. P. DenBaars, and J. S. Speck, ACS Photonics **7**(3), 554 (2020).
[12]S. Fujikawa, T. Ishiguro, K. Wang, W. Terashima, H. Fujishiro, and H. Hirayama, J. Cryst. Growth **510**, 47 (2019).
[13]Y. Wang, D. Dheeraj, Z. Liu, M. Liang, Y. Li, X. Yi, J. Wang, J. Li, and H. Weman, Cryst. Growth Des. **19**, 5516 (2019).
[14]I. Grigelionis and I. Kašalynas, Appl. Sci. **10**, 851 (2020).
[15]X. Sun, D. Li, Y. Chen, H. Song, H. Jiang, Z. Li, G. Miao, and Z. Zhang, CrystEngComm **15**, 6066 (2013).
[16]R. G. Banal, M. Funato, and Y. Kawakami, Appl. Phys. Lett. **92**, 241905 (2008).
[17]F. J. Xu, L. S. Zhang, N. Xie, M. X. Wang, Y. H. Sun, B. Y. Liu, W. K. Ge, X. Q. Wang, and B. Shen, CrystEngComm **21**, 2490 (2019).
[18]H. Miyake, G. Nishio, S. Suzuki, K. Hiramatsu, H. Fukuyama, J. Kaur, and N. Kuwano, Appl. Phys. Express **9**, 025501 (2016).
[19]J. Ben, X. Sun, Y. Jia, K. Jiang, Z. Shi, H. Liu, Y. Wang, C. Kai, Y. Wu, and D. Li, CrystEngComm **20**, 4623 (2018).
[20]M. Wang, F. Xu, N. Xie, Y. Sun, B. Liu, W. Ge, X. Kang, Z. Qin, X. Yang, X. Wang, and B. Shen, Appl. Phys. Lett. **114**, 112105 (2019).
[21]S. Xiao, R. Suzuki, H. Miyake, S. Harada, and T. Ujihara, J. Cryst. Growth **502**, 41 (2018).
[22]M. Benyoucef, M. Kuball, B. Beaumont, and V. Bousquet, Appl. Phys. Lett. **81**, 2370 (2002).
[23]W. M. Chen, P. J. McNally, J. Kanatharana, and D. Lowney, J. Mater. Sci. **14**, 283 (2003).
[24]M. Nemoz, R. Dagher, S. Matta, A. Michon, P. Vennéguès, and J. Brault, J. Cryst. Growth **461**, 10 (2017).
[25]H. Okumura, T. Kimoto, and J. Suda, Appl. Phys. Lett. **105**, 071603 (2014).
[26]D. Hull and D. J. Bacon, "Introduction to dislocations," *Movement of Dislocations* (Butterworth-Heinemann, MA, 2001), pp. 55–57.